

# Aging Studies for the Muon Detector of HERA-B

M. Danilov<sup>a</sup>, Yu. Gulitsky<sup>b</sup>, T. Kvaratschellia<sup>a</sup>, I. Tikhomirov<sup>a</sup>, M. Titov<sup>a,\*</sup>, Yu. Zaitsev<sup>a</sup>

<sup>a</sup>Institute of Theoretical and Experimental Physics (ITEP), 117259, Moscow, Russia

<sup>b</sup>Institute of High Energy Physics, Protvino, Russia

Presented by Maxim Titov

The severe radiation environment of the HERA-B experiment leads to a maximum accumulated charge on a wire, within the muon detector, of  $200 \frac{mC}{cm \text{ wire}}$ . For operation in this high-intensity environment, the main criteria for the gas choice turned out to be stability against aging. We report recent results of aging studies performed by irradiating aluminum proportional wire chambers filled with  $Ar/CF_4/CH_4$  (74:20:6),  $Ar/CF_4/CH_4$  (67:30:3),  $Ar/CF_4/CO_2$  (65:30:5)  $Ar/CF_4$  (70:30),  $CF_4/CH_4$  (90:10) and  $CF_4/CH_4$  (80:20) mixtures in three different experimental setups: laboratory conditions ( $Fe^{55}$  and  $Ru^{106}$  sources), a 100 MeV  $\alpha$ -beam and the high-rate HERA-B environment (secondaries from interactions of 920 GeV protons with target nucleus). Our experience shows that the aging rate depends not only on the total collected charge, but, in addition, on the mode of operation (high voltage and/or gas gain) and area of irradiation.

Effects of  $CF_4$  addition on aging performance of gaseous detectors are summarized. Possible application of these results for operation of large scale gaseous detectors in the high rate environment is discussed.

## 1. INTRODUCTION

The most recent developments in high-energy physics require a dramatic increase of radiation intensity encountered by gaseous detectors: from a few  $mC/cm/wire$  for standard radiation level detectors up to  $C/cm/wire$  for the new high-rate experiments of the LHC-era (HERA-B, LHC). The HERA-B experiment is a hadronic B-factory at DESY, Hamburg, where  $B$ -mesons are produced via interactions of 920 GeV beam halo protons with an internal target [1,2]. In order to produce a sufficient number of  $B$ -mesons, the HERA-B detector must operate at an extremely high  $pN$ -interaction rate of  $\sim 40$  MHz, which results in events with large charge and neutral multiplicities - up to several hundred particles every 96 ns - and a harsh radiation environment for the constituent detectors.

Addressing the needs of high-luminosity experiments aging studies should be also performed for muon detectors, known so far for low instantaneous rates and negligible radiation doses. At the

maximum cell occupancy in the HERA-B Muon System of 20 %, the event rate of  $pN$ -interactions of 10 MHz translates into a particle rate of 2 MHz integrated over the 3 m wire length. This rate is mostly due to  $\sim 1$  MeV  $\gamma$ 's that give rise to signals on average 3-4 times larger than from MIP's. The main objective of these studies was to prove that muon chambers are capable of operating up to  $600 \frac{mC}{cm \text{ wire}}$ , without loss in performance.

## 2. THE HERA-B MUON SYSTEM

The Muon Detector of the HERA-B, a large area gaseous detector with a total gas volume of  $8 m^3$ , consists of 1000 chamber modules read out with 30000 electronic readout channels. The overall area covered by chamber modules is  $800 m^2$ . Three different types of gas proportional chambers make up the muon system: tube, pad and pixel [3]. In this paper we present aging results only for a single layer tube chamber, which is a closed-cell proportional wire chamber made from an aluminum profile with 16 drift cells of  $14 \times 12 mm^2$  in cross section and a length of

\*Corresponding author. E-mail:titov@mail.desy.de

0.5 m [3]. A gold-plated tungsten wire of  $45 \mu\text{m}$  diameter is stretched inside each cell with a tension of 150 g and fixed mechanically in pins at the chamber end-caps made of noryl. An araldit is applied from outside the chamber in seams between aluminum profile and end-cap to provide a gas-tight seal. Fig. 1 shows the schematic drawing of the tube chamber. The gas flow within the chamber is serial from one cell to another.

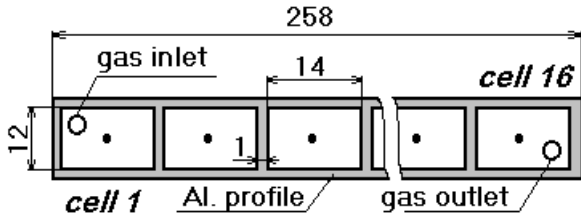


Figure 1. Schematic drawing of the single layer tube chamber.

### 2.1. Choice of Gas Mixture

Future high energy and high luminosity experiments pose a new challenge for gas mixtures, raising the requirement for their radiation hardness up to  $1 \frac{\text{C}}{\text{cm wire}}$  per year. Under these constraints only a limited choice of gases is available, and from the ‘conventional mixtures’ only  $Ar(Xe)/CO_2$  are demonstrated to tolerate such doses. Unfortunately, these mixtures are quite transparent for photons and have a low electron drift velocity, which limits their possible application for high-rates and large drift distances.

About twenty years ago,  $CF_4$  was proposed as the most attractive candidate for high-rate environments [4]-[6]. This is primarily due to the high-drift velocity, high primary ionization, low electron diffusion and resistance to aging [7]-[9]. Within the broad spectrum of gases, there is no gas mixture without  $CF_4$  that is able to tolerate doses  $\sim 10 \frac{\text{C}}{\text{cm wire}}$ . However, the  $CF_4$  molecule has a small quenching cross-sections of metastable  $Ar$ -states [10] and excited  $CF_4$  molecules emit photons from the far UV to the visible [11]. This results in an intolerable level of afterpulsing in  $Ar/CF_4$  gases even at moderate gas gains. Moreover,  $Ar(Xe)/CF_4$  mixtures have rather poor energy and spatial resolution

due to the dissociative electron attachment processes in  $CF_4$  [12]-[14]. The advantage of the enhanced drift velocity of  $CF_4$  for high-rate applications have been realized by the addition of one of the common quenchers (e.g.  $CO_2$ ,  $CH_4$ ) to  $CF_4$  or to  $Ar/CF_4$ . This can also ‘cool’ electrons to the extent that attachment does not occur. For example, addition of 10 % of  $CO_2$  to  $Ar/CF_4$  virtually eliminates the electron attachment in  $Ar/CF_4/CO_2$  (80:10:10) [5].

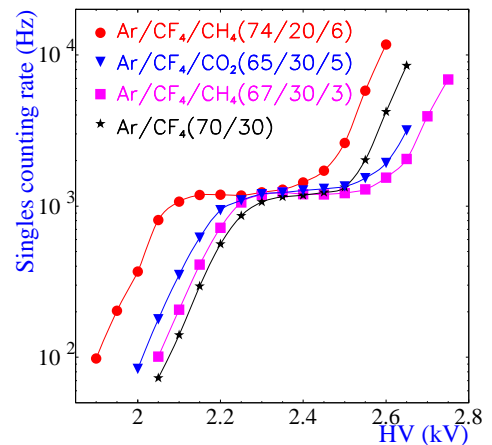


Figure 2. Singles counting rate vs HV measured in a 3 GeV  $e^-$  beam with an intensity  $\sim 1$  kHz.

Strong restrictions on the gaseous medium to be used in the HERA-B muon chambers are imposed by operating conditions. In addition to a large integrated radiation dose, chamber signals, which are used to form the trigger, must be collected in less than the 96 ns between HERA bunch crossings. Our studies [15,16] have shown that the properties of several non-flammable fast mixtures:  $Ar/CF_4/CH_4$  (74:20:6),  $Ar/CF_4/CH_4$  (67:30:3) and  $Ar/CF_4/CO_2$  (65:30:5) ensure efficient ( $> 99\%$  within 96 ns) and stable (wide counting rate plateau) operation for double layer tube chamber (see Fig. 2). These results also confirm that significant loss of ionization electrons before avalanche development (using [13], we estimated the electron attachment coefficient  $k$ , defined as the ratio of the number of primary ionization electrons to the number of those reaching the anode, to be  $k=5$  for  $Ar/CF_4/CH_4$  (67:30:3) and

$k=4$  for  $Ar/CF_4/CO_2$  (65:30:5)) does not affect tube chamber performance.

However, the main criteria for the choice of the gas turned out to be the stability against aging.

### 3. AGING RESULTS FROM LABORATORY TESTS

Since experience from laboratory tests, where operating conditions are much better controlled, can be used to understand some general principles and might help to implement these results successfully in large chambers, initially we have carried out study of the aging properties of  $Ar/CF_4/CH_4$  (74:20:6) mixture exposed to  $Fe^{55}$  source, and of  $Ar/CF_4/CH_4$  (67:30:3) and  $Ar/CF_4/CO_2$  (65:30:5) mixtures, both irradiated with an  $Ru^{106}$  source, up to a total radiation dose of  $2 \frac{C}{cm \text{ wire}}$ . Below, only the most important results regarding laboratory studies are given; more details can be obtained from papers [16,17].

In each test, a single cell of the proportional tube chamber was used; the irradiated area was limited by a collimator to about 30 mm of the wire for  $Fe^{55}$  source and to 10 mm for  $Ru^{106}$  source. The gas flow rate was 1 l/h. The high voltages used during the aging studies ( $Ar/CF_4/CH_4$  (74:20:6) - 2.65 kV,  $Ar/CF_4/CH_4$  (67:30:3) - 2.69 kV,  $Ar/CF_4/CO_2$  (65:30:5) - 2.79 kV) exceeded those for the proportional mode operation; the current densities were 700-1200 nA/cm. Nominal HV for the tube chamber (see Fig 2), corresponding to effective gas gain of  $\sim 3 \times 10^4$ , are the following:  $Ar/CF_4/CH_4$  (74:20:6)-2.25 kV,  $Ar/CF_4/CH_4$  (67:30:3)-2.45 kV,  $Ar/CF_4/CO_2$  (65:30:5)-2.4 kV.

Fig. 3 shows the ratio of  $Fe^{55}$  peak positions, measured at irradiated and reference spots as a function of the accumulated charge. For the  $Ar/CF_4/CH_4$  (74:20:6) mixture, the relative mean amplitude  $A_{irrad}/A_{reference}$  monotonically dropped to about 85 % of the initial value, after the radiation dose of 2 C/cm of the wire, corresponding to  $R = -\frac{1}{G} \frac{dG}{dQ}$  (% per C/cm)  $\sim 8$  % per C/cm. Irradiation with a  $Ru^{106}$  source showed that tube chambers filled with  $Ar/CF_4/CH_4$ (67:30:3) and

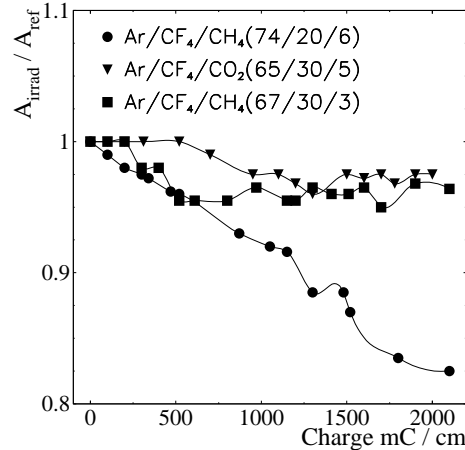


Figure 3. Ratio of  $Fe^{55}$  peak positions at irradiated and reference spots as a function of the accumulated charge.

$Ar/CF_4/CO_2$ (65:30:5) are able to tolerate doses up to 2 C/cm per wire with negligible aging effects. Such an aging behavior make these gases suitable candidates for the long-term operation of muon chambers.

### 4. AGING STUDIES IN A 100 MeV $\alpha$ -BEAM

#### 4.1. Aging in $Ar/CF_4/CH_4$ (74:20:6)

Radiation tests with an  $Ar/CF_4/CH_4$  (74:20:6) mixture have been carried out in a 100 MeV  $\alpha$ -beam of the cyclotron in the Forschungszentrum Karlsruhe. Due to the small range of the 100 MeV  $\alpha$ 's in aluminum, the thickness of the Al-wall in the central part of the chamber (exposed to uniform  $\alpha$ -beam of  $8 \times 8 \text{ cm}^2$ ) was reduced to 200  $\mu\text{m}$ . The gas flow was 6 l/h. Stainless-steel tubes were used for a gas supply lines. The high voltage was set to 2.35 kV. The radiation intensity varied during the aging studies by a factor of 3; the current densities were in the range from 250 nA/cm up to 750 nA/cm.

In sharp contrast to laboratory tests, after the first 30 hours of  $\alpha$ -beam exposure, which resulted in a collected charge of  $\sim 60 \frac{mC}{cm \text{ wire}}$ , severe anode aging was observed in the irradiated regions of the wires. The average gas gain loss for one of the wires in the exposed area was found to be  $R \sim 850$  % per C/cm, while the  $Fe^{55}$  spectra

in the non-irradiated part remained unchanged. Since that time, this wire was disconnected from the high voltage; all others were irradiated up to  $\sim 280 \frac{mC}{cm \text{ wire}}$ . The observed aging effects for all wires during exposure to  $\alpha$ 's were quite similar: continuous reduction of the  $Fe^{55}$  peak value, large increase in the single counting rate above the actual  $\alpha$ -beam intensity, dark current and the monotonic drop in anode current [16].

After the  $\alpha$ -beam tests all wires exposed to  $\sim 280 \frac{mC}{cm \text{ wire}}$  were heavily damaged (efficiency to MIP's was  $\sim 10\%$  at HV=2.25 kV). Observation of all damaged wires under a microscope showed vertically structured black deposits or 'whiskers' within the irradiated area with lengths up to  $50 \mu m$  (see Fig. 4)

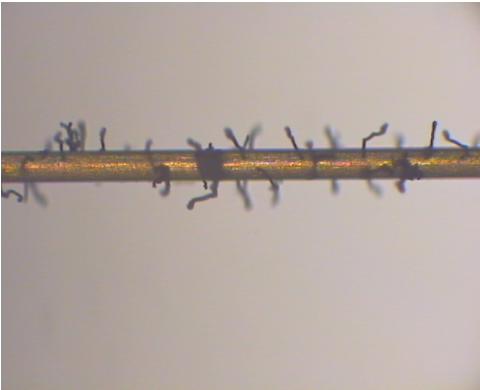


Figure 4. Deposits on the anode wire after exposure to  $\alpha$ 's in  $Ar/CF_4/CH_4$  (74:20:6).

In addition, all wires and cathodes were also taken for surface analysis at 'Digital Analytical Scanning Microscope JSM-6400'. The scanning electron microscope (SEM) yields information on the morphology of the wire surface by imaging with scattered and secondary electrons, and energy dispersive X-ray spectroscopy (EDX) analysis gives the atomic composition of the surface material. In our tests, micrographs of anode wires were mostly taken at SEM accelerating voltage 20 kV (sometimes - 5 kV), while cathodes were analyzed at 5 kV. The increased sensitivity to surface deposits at 5 kV is due to the reduced penetration of the lower energy primary electrons.

SEM/EDX analysis of all heavily aged wires revealed deposits containing carbon and fluorine as the only detectable elements (hydrogen is not detectable). Moreover, carbon and fluorine signals were also identified in the irradiated regions free of 'whiskers', together with Au signal from the wire. (Wire exposed to  $60 \frac{mC}{cm \text{ wire}}$  had a fewer whiskers and less amount of carbon and fluorine on the Au surface). New wires and wires which were exposed to the irradiated gas, but not irradiated themselves, showed peaks only from Au. Some layer consisting of C and O was observed on the irradiated cathodes.

The aging rate in our studies for  $Ar/CF_4/CH_4$  (74:20:6) gas mixture was found to be at least two orders of magnitude higher in a 100 MeV  $\alpha$ 's than in laboratory tests with  $Fe^{55}$  X-rays. The difference between these results could be partially attributed to the larger total charge released from  $\alpha$ 's in the chamber cell, larger size of the irradiated area or some other variations in the operating parameters. From these results, it is evident that from the accumulated charge alone, it is not possible to combine the data from the different radiation sources into one consistent model. The fast anode aging observed with  $\alpha$ 's ruled out  $Ar/CF_4/CH_4$  (74:20:6) as a candidate for operation in the HERA-B environment, where at least part of the ionization comes from heavily ionizing particle. Therefore, further systematic R&D aging tests were performed in the realistic (both in particle composition and in ionization density) HERA-B environment.

## 5. AGING STUDIES IN A HERA-B ENVIRONMENT

To test the aging properties in realistic environment (secondaries from interactions of 920 GeV protons with target nucleus), three tube chambers were placed behind the HERA-B electromagnetic calorimeter, where particle rates up to 10 times higher than in the muon system. For the aging tests with  $Ar/CF_4/CH_4$  (67:30:3) and  $Ar/CF_4/CO_2$  (65:30:5) mixtures, two of the chambers were subdivided to allow groups of anode wires (zones) to be operated at five different high voltages. The gas flow rate was  $3 \text{ l/h}$

(2 chamber volumes/ $h$ ). Fig. 5 shows a simple schematic representation of the experimental setup, numbering scheme for the wires, and summarizes the operating conditions. Between any two zones there was a reference wire for which high voltage was not applied. A decrease in particle flux together with increase in high voltage with the distance from the proton beam led to comparable accumulated charges in HV-zones 2,3,4,5. Due to variations in the rate of  $pN$ -interactions during HERA-B operation, the current densities varied in aging studies by a factor of 4. The third chamber was subdivided into 4 zones, each containing two or three wires, as shown in Fig. 5. Radiation studies with mixtures  $CF_4/CH_4$  (90:10),  $CF_4/CH_4$  (80:20),  $Ar/CF_4$  (70:30) were performed on different wires in order to investigate the influence of construction materials and possible pollutant substances in the gas system, as well as water addition and cathode cleanliness, on the aging performance.

For each chamber a pre-mixed gas was transported by a 150 m stainless steel tube followed by a polyamid tube connected directly to the chamber inlet. The addition of water to the gas was done indirectly, by varying the length of the polyamid tube, which is transparent to  $H_2O$ , for a fixed flow rate [17]. The gas inlet was connected to wire N1, and the gas outlet to wire N16. The gas outlet of the chamber was connected via a 50 m stainless steel tube to the input of a gas chromatograph, which was used to analyze the concentration of species ( $Ar$ ,  $CF_4$ ,  $CH_4$ ,  $CO_2$ ,  $N_2$ ,  $O_2$ ,  $H_2O$ ) in the effluent gas stream. Usually, measured concentrations of  $N_2$  and  $O_2$  were at the level of 150-250 ppm.

Typically once per month chamber characteristics were studied in a 3 GeV electron beam at DESY with an intensity  $\sim 1 \text{ kHz}/\text{cm}^2$ . A reduction in efficiency at a nominal HV measured with electrons at different locations along the wire was used as the main information about the gas gain loss. In addition, the appearance of several other phenomena for a particular group of anode wires during exposure in HERA-B clearly indicated the onset of aging effects: dark current, persistence of current after the beam switch-off (Malter effect) and special 'switch-on' current behavior (decrease

	Chamber №1 Ar/CF <sub>4</sub> /CH <sub>4</sub> (67:30:3)		Chamber №2 Ar/CF <sub>4</sub> /CO <sub>2</sub> (65:30:5)	
HV	Wires	Current density	Wires	Current density
Zone 1: 2.25kV	1,2	40 nA/cm	1,2	50 nA/cm
Zone 2: 2.50kV	4,5	150 nA/cm	4,5	210 nA/cm
Zone 3: 2.55kV	7,8	150 nA/cm	7,8	210 nA/cm
Zone 4: 2.60kV	10,11	150 nA/cm	10,11	210 nA/cm
Zone 5: 2.65kV	13,14,15	200 nA/cm	13,14,15	270 nA/cm
Reference wires	3,6,9,12,16	0	3,6,9,12,16	0
Chamber №3				
CF <sub>4</sub> /CH <sub>4</sub> (90:10) + 600ppm H <sub>2</sub> O				
3.0 kV	1,2	200 nA/cm		
CF <sub>4</sub> /CH <sub>4</sub> (80:20) + 600ppm H <sub>2</sub> O				
3.0 kV	7,8,9	150 nA/cm		
CF <sub>4</sub> /CH <sub>4</sub> (80:20)				
3.0 kV	11,12,13	100 nA/cm		
Ar/CH <sub>4</sub> (70:30)				
2.60 kV	15,16	150 nA/cm		

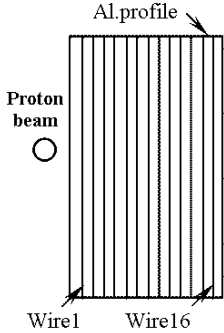


Figure 5. Schematic representation of the experimental setup and summary of operating conditions (high voltages and average current densities).

in the anode current after high voltage is applied, since a certain time is necessary to establish the equilibrium charge density on the aged wire surface) [18–20]. Finally, for all aged wires operated with an  $Ar/CF_4/CH_4$  mixture in the HERA-B environment the operating current was dependent upon the gas flow rate (an increase of gas flow led to an increase in the anode current); this effect will be discussed in Section 6.

Below, the most important results of our studies are presented; more experimental details can be found in [21].

### 5.1. Aging in $Ar/CF_4/CH_4$ (67:30:3)

Due to the expected dominant role of hydrocarbon polymerization in  $CH_4/CH_4$  gases [22], and the reduced  $CH_4$  content in  $Ar/CF_4/CH_4$  (67:30:3) better aging properties of this mixture, compared to  $Ar/CF_4/CH_4$  (74:20:6), were ex-

pected.

Since water is believed to prevent polymerization of hydrocarbons, we used 500 ppm of  $H_2O$  in the first aging run. First results in the HERA-B environment showed that the aging properties of  $Ar/CF_4/CH_4$  (67:30:3) + 500 ppm  $H_2O$  mixture depend on the gas amplification/high voltage and area of irradiation.

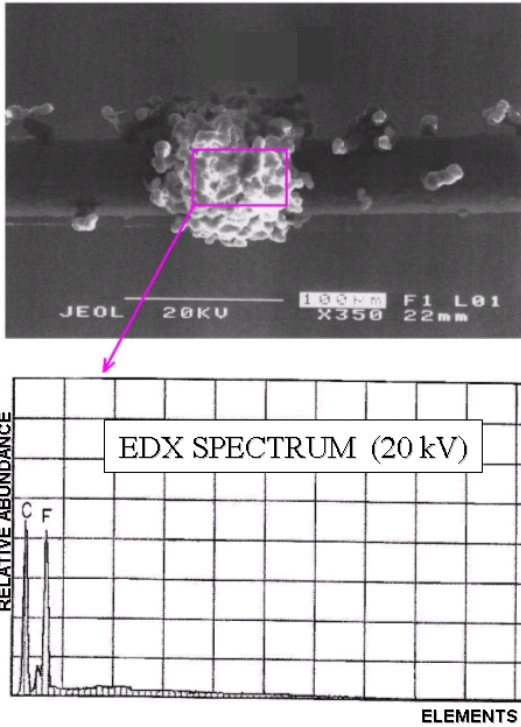


Figure 6. SEM/EDX examination of the wire N15, irradiated at 2.65 kV in an  $Ar/CF_4/CH_4$  (67:30:3) + 500 ppm  $H_2O$ , showed deposits containing carbon and fluorine as the only detectable elements (hydrogen is not detectable).

Electron beam tests revealed rapid anode aging effects for wires N14,N15 operated at 2.65 kV after  $\sim 25 \frac{mC}{cm \cdot wire}$ ; after a charge of  $\sim 100 \frac{mC}{cm \cdot wire}$  all three wires N13-N15 in zone 5 showed gain reduction. For the wires irradiated at 2.6 kV aging effects appeared after  $\sim 80 \frac{mC}{cm \cdot wire}$  for the wire N11, while at a radiation dose of  $170 \frac{mC}{cm \cdot wire}$  efficiency loss was observed in both cells N10,N11. In addition to a gain reduction for the wires

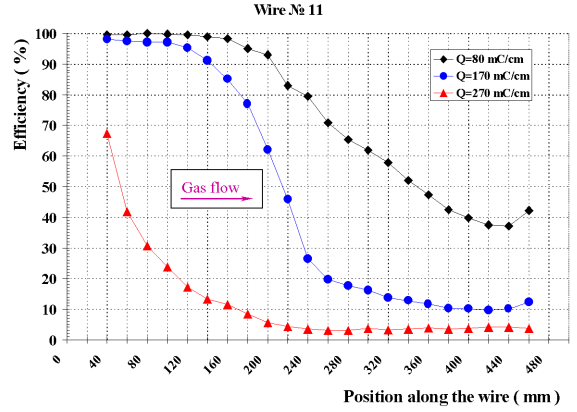


Figure 7. Efficiency profiles along wire N11 for different accumulated charges:  $80 \frac{mC}{cm \cdot wire}$ ,  $170 \frac{mC}{cm \cdot wire}$ ,  $270 \frac{mC}{cm \cdot wire}$  in an  $Ar/CF_4/CH_4$  (67:30:3) + 500 ppm  $H_2O$ . Efficiency of the 'reference wire' is  $> 99\%$  at HV=2.4 kV.

at  $HV \geq 2.6$  kV, their operation at HERA-B was accompanied by appearance of dark current after the HERA beam switch-off. The aging test with  $Ar/CF_4/CH_4$  (67:30:3) + 500 ppm  $H_2O$  was carried out up to an accumulated charge of  $\sim 400 \frac{mC}{cm \cdot wire}$  for the wires in HV zones 2,3,4 ( $\sim 200 \frac{mC}{cm \cdot wire}$  in zone 5,  $\sim 100 \frac{mC}{cm \cdot wire}$  in zone 1). After the first aging run, no gain loss was observed for most wires N1-N8 specimens, except several distinct spots (with sizes of a few cm) on wires N5,N7,N8, where drop in efficiency ( $\sim 90-98\%$  at 2.4 kV) was found. EDX analysis of all aged wires at  $HV \geq 2.6$  kV revealed deposits containing carbon and fluorine as the only detectable elements (see Fig. 6). In addition, two other interesting phenomena were observed for the aged wires at  $HV \geq 2.6$  kV:

- Progressive deterioration of the gas gain in the direction of the serial gas flow
- The fluorine-to-carbon ratio in the polymer coating increased in the gas flow direction

Fig. 7 shows an example of how the efficiency profile for wire N11 developed in the direction of gas flow (with increasing usage of gas) as a function of accumulated charge.

In the second aging run we increased the water content (1400 ppm) in an  $Ar/CF_4/CH_4$

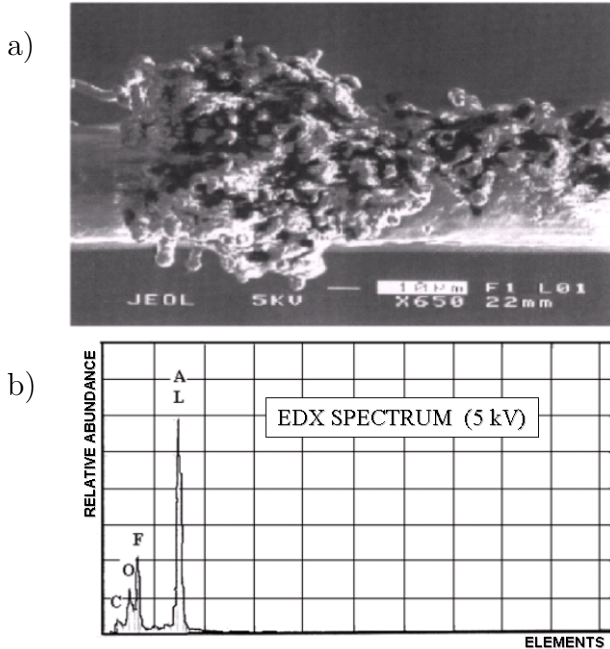


Figure 8. a) Typical 'whiskers' on the anode wire N5 and b) EDX analysis of the cathode in the same cell, irradiated at 2.5 kV in an  $Ar/CF_4/CH_4$  (67:30:3) after the third aging run.

(67:30:3), and continued tests using previously irradiated wires in HV zones 1,2,3. During three months of operation, approximately  $400 \frac{mC}{cm \cdot wire}$  were accumulated for wires in zones 2,3 ( $100 \frac{mC}{cm \cdot wire}$  in zone 1) in addition to the charge collected in the first run. At the end of the second run (total radiation dose was about  $800 \frac{mC}{cm \cdot wire}$  in zones 2,3) all inefficient spots on wires N5,N7,N8 had vanished. Subsequent EDX examination of the anode wires N1,N4,N5,N7,N8 revealed only *Au* signal thus confirming the absence of the polymer coating. Small amount of *Si*-contamination was identified on wire N2, which operated at the lowest current density ( $\leq 10 \text{ nA/cm}$ ). The absence of *Si*-containing deposits on all other aged wires in  $Ar/CF_4/CH_4$  indicates that *Si*-polymerization was not a dominant aging process in our tests.

Before the next aging run chamber cells that had been previously aged were restrung with new anode wires. We started this run using same

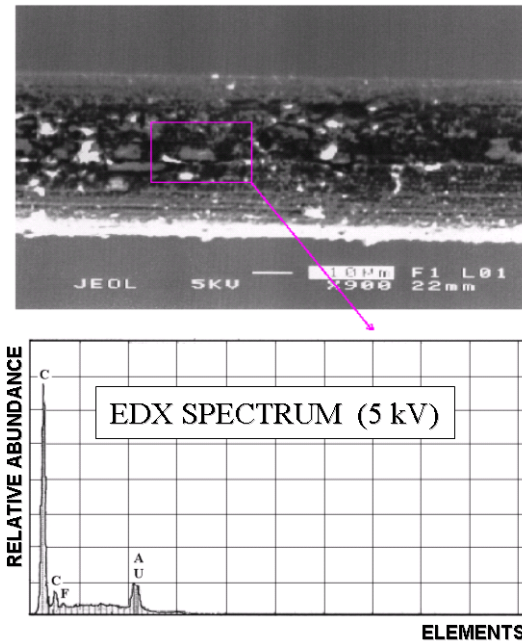


Figure 9. SEM/EDX imaging of the wire N1 irradiated at 2.25 kV in an  $Ar/CF_4/CH_4$  (67:30:3) after the third aging run.

mixture  $Ar/CF_4/CH_4$  (67:30:3) + 1400 ppm of  $H_2O$  and collected approximately  $80 \frac{mC}{cm \cdot wire}$  for the wires N4,N5,N6 operated at 2.5 kV and  $40 \frac{mC}{cm \cdot wire}$  for the wires N1,N2 at 2.25 kV. During this time no aging effects were observed for all irradiated wires. At this point we exchanged polyamid tubes with stainless-steel ones, flushed a chamber long time until the water content at the chamber outlet became  $< 150 \text{ ppm}$ , and then continued aging test. After a dose of only  $\sim 30 \frac{mC}{cm \cdot wire}$ , both Malter current and steadily decreasing anode current have been observed for the wires N4,N5,N6. These effects were not seen for wires N1,N2 until the end of exposure in HERA-B. During the third aging run with  $Ar/CF_4/CH_4$  (67:30:3) without water ( $H_2O < 150 \text{ ppm}$ ) we collected  $\sim 70 \frac{mC}{cm \cdot wire}$  for the wires at HV=2.5 kV and  $\sim 20 \frac{mC}{cm \cdot wire}$  at HV=2.25 kV. Subsequent studies in an electron beam confirmed dramatical gain reduction for all wires operated at 2.5 kV with efficiency decreasing in the direction of the serial gas flow. Fig. 8a presents typical micrographs of the shaped growth deposits on the

anode wire N5, consisting only of *C* and *F* elements, which are very similar to those observed with  $Ar/CF_4/CH_4$  (67:30:3) + 500 ppm  $H_2O$  at  $HV \geq 2.6$  kV. EDX analysis of irradiated cathode in the same cell revealed significant amount of *C*, *F* and *O* on aluminum surface (see Fig. 8b). Some gain loss for wire N1 was also observed in an electron beam. However, in contrast to deposits on other aged wires, EDX spectrum of wire N1 is dominated by intense C peak without incorporation of *F* into a polymer matrix (see Fig. 9). No change in performance was observed for wire N2.

These results clearly ruled out the possibility to use  $Ar/CF_4/CH_4$  (67:30:3) at high ionization densities due to the strong dependence of aging properties on high voltage and size of irradiation area, although under some conditions (gas gain <  $10^5$ , water addition  $\sim 1500$  ppm) no aging effects were seen up to a dose of  $800 \frac{mC}{cm \cdot wire}$ .

### 5.2. Aging in $Ar/CF_4/CO_2$ (65:30:5)

Radiation tests with  $Ar/CF_4/CO_2$  (65:30:5) + 1000 ppm of  $H_2O$  were performed up to the total collected charge of  $\sim 700 \frac{mC}{cm \cdot wire}$  in HV zones 2-5 ( $\sim 170 \frac{mC}{cm \cdot wire}$  in zone 1). No aging effects were seen: nor were persistent currents after the beam switch-off or other residual currents detectable for all exposed wires in HERA-B. No loss in performance (gain reduction) was confirmed during the monthly electron beam tests for all irradiated wires up to the total radiation dose.

After the chamber was disassembled, the appearance of a few wire specimens was slightly more black than of a new ones. However, SEM/EDX examination of irradiated wires revealed extremely clean *Au* surfaces (wire N5, Fig. 10) with only a few point-like deposits (*Si, Al*) with sizes of 1-2  $\mu m$  that did not cause local inefficiencies. Interestingly, despite local deterioration of the smooth wire surface (wire N13, Fig. 10), its elemental composition is also dominated by *Au* peak and there is no evidence of other chemical elements.

An analysis of cathode surfaces revealed trace amounts of *C*, *O* and *F* in cells operated at 2.65 kV (see Fig. 11). However, these fluorine-based deposits did not result in cathode-related aging effects - self-sustained currents or loss of

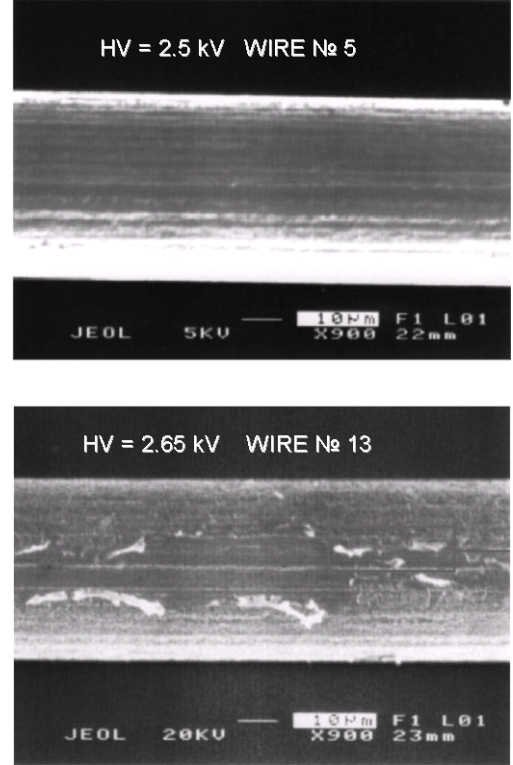


Figure 10. SEM imaging of the wires irradiated at 2.5 kV (wire N5) and at 2.65 kV (wire N13) in an  $Ar/CF_4/CO_2$  (65:30:5) + 1000 ppm of  $H_2O$  after a dose of  $700 \frac{mC}{cm \cdot wire}$ .

gas gain. (Trace fluorocarbon deposits on cathodes from pure  $CF_4$  discharges could be resistive enough to cause a voltage drop on the cathode, which in turn lowers the gas gain [22]). For cells irradiated at 2.55 kV the relative abundances of *C*, *O*, *F* on aluminum surface were greatly reduced, while for a baseline high voltage exposed cathodes were almost indistinguishable from the reference ones (see Fig. 11).

Therefore,  $Ar/CF_4/CO_2$ (65:30:5) + 1000 ppm  $H_2O$  mixture is currently used for the muon chamber operation.

### 5.3. Aging in $Ar/CF_4$ (70:30)

In wire chambers, hydrocarbon free mixtures are much more resistant to polymerization effects than gases containing hydrocarbons. Our results also demonstrate that the tube chamber lifetime

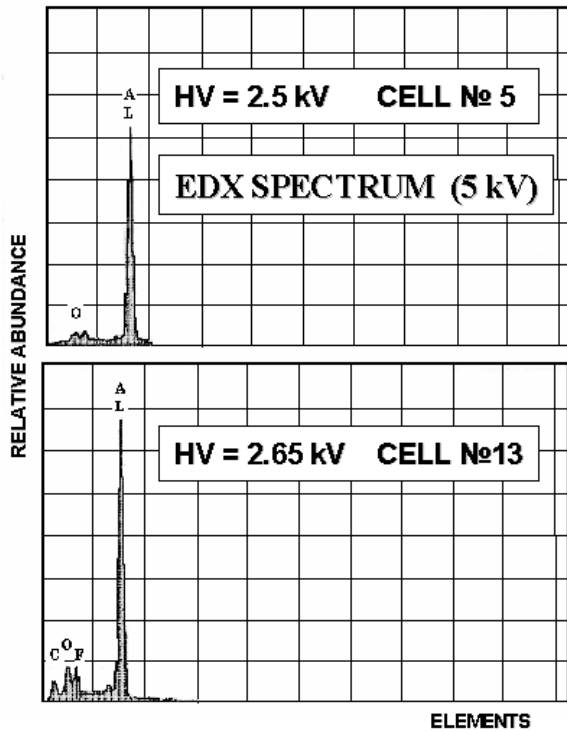


Figure 11. EDX of cathode cells irradiated at 2.5 kV (cell N5) and at 2.65 kV (cell N13) in an  $Ar/CF_4/CO_2$  (65:30:5) + 1000 ppm of  $H_2O$  up to a dose of  $700 \frac{mC}{cm \cdot wire}$ .

changes dramatically by replacing 3 % or 6 % of  $CH_4$  by 5 % of  $CO_2$  in the  $Ar/CF_4$  mixture. Correspondingly, this difference can be solely attributed to the change in the gas phase and gas surface chemical reactions in avalanches, after replacement of a quencher  $CH_4$  by  $CO_2$ .

It is also worthwhile to note that in aging studies for the ATLAS muon drift tubes the cleanliness of aluminum cathodes was identified as an important factor for the lifetime even in the hydrocarbon free mixture  $Ar/CO_2/N_2$  (90:5:5)+1200 ppm  $H_2O$ . Hydrocarbon greases from the production process are not always completely removed during the cleaning procedure of the aluminum tubes. Sputtering by UV-photons from wire avalanches can lead to the removal of non-volatile hydrocarbons from the cathode,

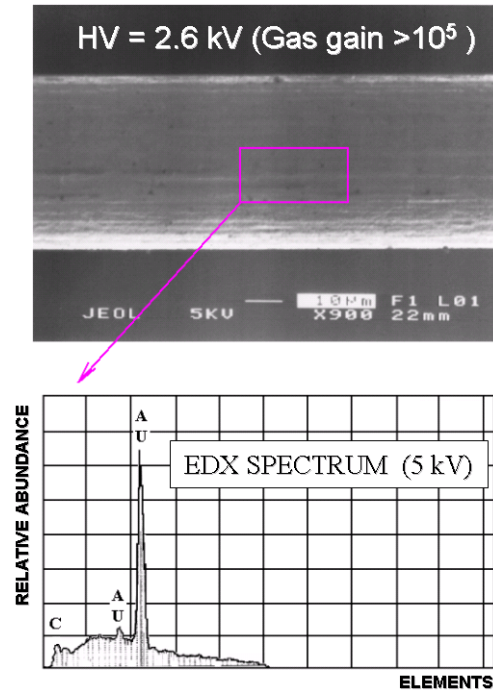


Figure 12. SEM/EDX examination of wire N16, irradiated in an  $Ar/CF_4$  (70:30) mixture after accumulated charge  $\sim 70 \frac{mC}{cm \cdot wire}$ .

which then drift and stick to the wires, or can initiate/promote the polymerization processes in the chamber [23].

Aging studies with  $Ar/CF_4$ , which is expected to have a strong etching capability, were carried out in order to exclude the effect of cathode cleanliness and possible pollutants present in the gas on aging performance and to confirm that fast aging in  $Ar/CF_4/CH_4$  appears only when  $CH_4$  is added to  $Ar/CF_4$ .

Radiation tests with an  $Ar/CF_4$  (70:30) were performed on two wires N15, N16 up to collected charge  $\sim 70 \frac{mC}{cm \cdot wire}$ . Only stainless steel tubes were used for gas supply lines that excluded presence of  $H_2O$ ; the gas flow rate was 1.5 l/h. The high voltage was set to 2.6 kV, where the rate of spurious pulses is very large (see Fig. 2), to force the chamber to discharge. The average current density was  $\sim 150$  nA/cm. No anode/cathode aging (neither persistence of current after beam switch-off nor changes in current density normal-

ized to the HERA-B interaction rate) was observed up to the end of our tests. Further electron beam studies confirmed no local loss of gas gain for both wires. The appearance of some wire specimens after exposure in  $Ar/CF_4$  was slightly more black than of new ones. However, SEM/EDX analysis revealed clean  $Au$  wire surfaces, with negligible traces of  $C$  identified only at 5 kV SEM voltage (see Fig. 12). EDX analysis of irradiated cathodes revealed minor traces of  $C$  and  $F$ .

#### 5.4. Aging in $CF_4/CH_4$ (90:10)

Finally, in order to find a link between divergent results in  $CF_4$ /hydrocarbon mixtures (see also section 7), and to compare the aging properties of  $CF_4/CH_4$  and  $Ar/CF_4/CH_4$  mixtures in the HERA-B environment, we have carried out aging studies with  $CF_4/CH_4$  (90:10) and  $CF_4/CH_4$  (80:20) gases.

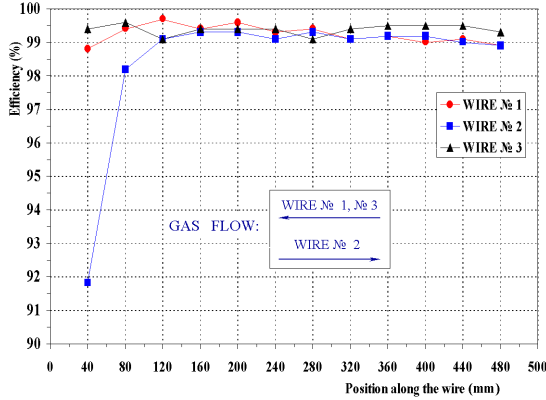


Figure 13. Efficiency profiles along wires N1,N2 measured in an electron beam, after a charge of  $\sim 370 \frac{mC}{cm \cdot wire}$  in an  $CF_4/CH_4$  (90:10) + 600 ppm  $H_2O$ . Efficiency of reference wire N3  $\geq 99\%$ .

Radiation tests with  $CF_4/CH_4$  (90:10) + 600 ppm  $H_2O$  mixture were performed on wires N1,N2 up to collected charge  $\sim 370 \frac{mC}{cm \cdot wire}$ . The flow rate was 1.5 l/h. The operating voltage was 3.0 kV, the average current density 200 nA/cm. No anode/cathode aging (dark current or changes in average current density) was observed during exposure in HERA-B. At the end of run, electron

beam tests revealed no gain loss for most wire specimens, except a region  $\sim 4$  cm of wire N2 (near one of the chamber end-caps), where a significant local inefficiency was found (see Fig. 13). Unfortunately, we were not able to perform EDX analysis of this region due to technical reasons; for all other wire specimens only a clean  $Au$  signal was observed. No layer of deposits was observed on the irradiated cathode surfaces.

#### 5.5. Aging in $CF_4/CH_4$ (80:20)

We have studied the aging properties of a  $CF_4/CH_4$ (80:20) mixture: 1) with 600 ppm  $H_2O$  and 2) without  $H_2O$ .

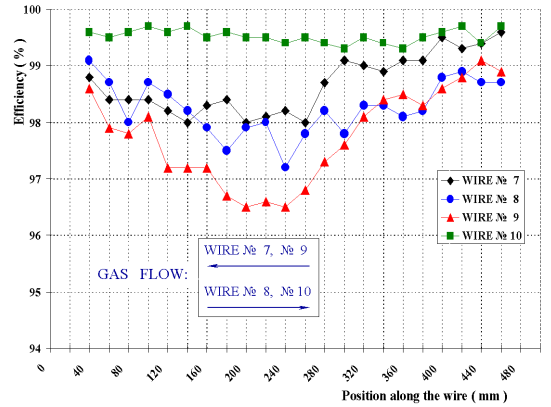


Figure 14. Efficiency profiles along wires N7,N8,N9, measured in an electron beam, after a charge of  $\sim 170 \frac{mC}{cm \cdot wire}$  in an  $CF_4/CH_4$ (80:20) + 600 ppm  $H_2O$ . Efficiency of reference wire N10 is  $\geq 99\%$ .

Radiation tests with a  $CF_4/CH_4$ (80:20) + 600 ppm  $H_2O$  were performed on wires N7,N8,N9 up to collected charge  $\sim 170 \frac{mC}{cm \cdot wire}$ . The flow rate was 1.5 l/h. The operating voltage was 3.0 kV, the average current density 150 nA/cm. Neither dark currents nor changes in average current density were observed up to the end of exposure in HERA-B. However, scanning along the wires in an electron beam revealed efficiency loss for all irradiated wires (see Fig 14). It has to be noted, though, that the observed gain reduction only slightly increases in the direction of the serial gas flow (from wire N7 to N9) and is much more

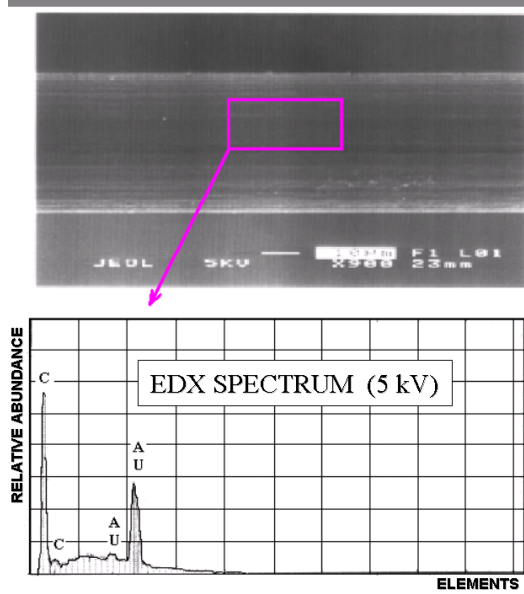


Figure 15. SEM/EDX analysis of the wire N8, irradiated in an  $CF_4/CH_4(80:20) + 600 \text{ ppm } H_2O$  after a radiation dose of  $170 \frac{mC}{cm \cdot wire}$ .

severe in the center of each wire ( $x \sim 250 \text{ cm}$ ), where the radiation intensity was the highest (see Fig. 14). Subsequent EDX analysis revealed presence of  $C$  contamination on irradiated wires surface (see Fig. 15). It is notable that the deposits are carbonaceous; the absence of fluorine indicates that they are formed from the  $CH_4$ , without incorporation of  $CF_x$  fragments. Only negligible amounts of  $C$ ,  $O$  and  $F$  were identified on irradiated cathodes.

Radiation tests with a  $CF_4/CH_4(80:20)$  mixture without water were performed on wires N11,N12,N13 up to  $\sim 40 \frac{mC}{cm \cdot wire}$ . All operating conditions were kept as before. Due to the large distance from proton beam for wires N11,N12,N13, the average current density was lower  $\sim 100 \text{ nA/cm}$ . During exposure, we have not noticed any anode/cathode aging effects; no gain reduction for all irradiated wires was confirmed later in electron beam tests.

## 6. 'Transient' aging effects

Correlated to the observation of the gain reduction and appearance of persistent dark current for the 'aged' wires in an  $Ar/CF_4/CH_4$ , we have also observed a sizeable dependence of the anode current from the gas flow rate. This phenomena was progressing with degree of the anode wire aging, but have never been observed in our studies for the wires without gain reduction.

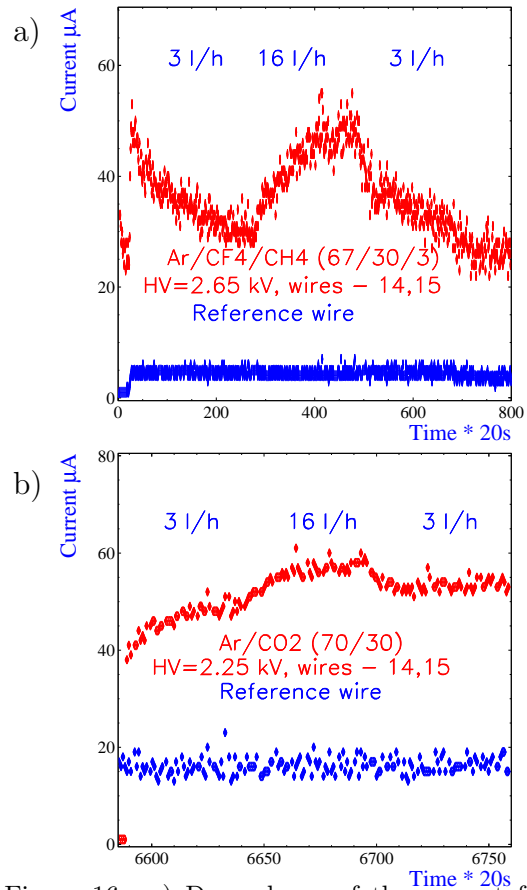


Figure 16. a) Dependence of the current from the gas flow rate for the partially 'aged' wires N14,N15 irradiated at 2.65 kV (top curve) and for the reference (non-aged) wires N1,N2 operated at 2.25 kV (bottom curve) in an  $Ar/CF_4/CH_4$  (67:30:3); b) Dependence of the current from the gas flow rate, in the same chamber filled with  $Ar/CO_2$  (70:30), for the 'aged' wires N14,N15 (top curve) and for the reference wires N1,N2 (bottom curve).

After switching on the high voltage on the wires N14, N15, showing signs of anode and cathode aging in an  $Ar/CF_4/CH_4$ , an exponential decay in the current reaching a plateau value was usually observed (see Fig. 16a). The increase in the gas flow from 3 l/h up to 16 l/h markedly restored the anode current to its initial value with a characteristic time corresponding approximately to one gas volume exchange of the chamber. However, as the gas flow was decreased again to 3 l/h the anode current drifted exponentially to its plateau value. When, in the next run, the same chamber was irradiated with a fluorine-free gas  $Ar/CO_2$  (70:30) the dependence of current from the flow rate was marginally visible, but rather some increase in the current (Malter effect) was seen in the aged cells (see Fig. 16b). The same measurements carried out with reference cells did not show any current variations, thus confirming constant radiation intensity during these experiments.

We think that this observation is another indication of generation of some neutral but stable electronegative radicals in  $CF_4$ -mixtures [24–26], which can be easily blown away by an appropriate gas flow. At a small gas flow, these polarizable molecules can be attracted to the anode wire and will modify the local charge density distribution near the insulating ('aged') sense-wire surface.

## 7. EXPERIENCE WITH $CF_4$ -BASED OPERATION

### 7.1. Plasma processing

While plasma characteristics (low pressure, rf) differ from those of wire chambers (1 atm, dc), some useful hints of traditional plasma chemistry [27–29] proved to be qualitatively applicable to the field of gaseous detectors (eg. a role of oxygen-based additives and  $CF_4$ ) [22,23,30,31].

The basic principle of plasma polymerization is that both polymer-forming species and species that cause ablation (physical or chemical etching) may be created in the plasma of the original gas and the extent of the process and the dominating mechanism vary with the types of gases and the discharge conditions. The significance of this concept is fully established for perfluorocarbons ( $CF_4$ ,  $C_2F_6$ ), which represent the most

extreme case of ablation competing with polymer formation. Actually,  $CF_4$ -based gases are used for both etching and deposition processes. The addition of oxygenated species shifts the chemistry of  $CF_4$  plasmas towards etching, while depending upon the amount of  $H_2$  added to  $CF_4$ , the balance between polymerization and etching can be controlled [27,28].

The dissociative products of  $CF_4$  and  $O_2$  are the most desirable active species for the plasma etching processes [32–35]. The addition of  $O_2$  to  $CF_4$  also produces a marked increase in the free fluorine atoms, which are suggested to be the principal etchant of silicon [33].

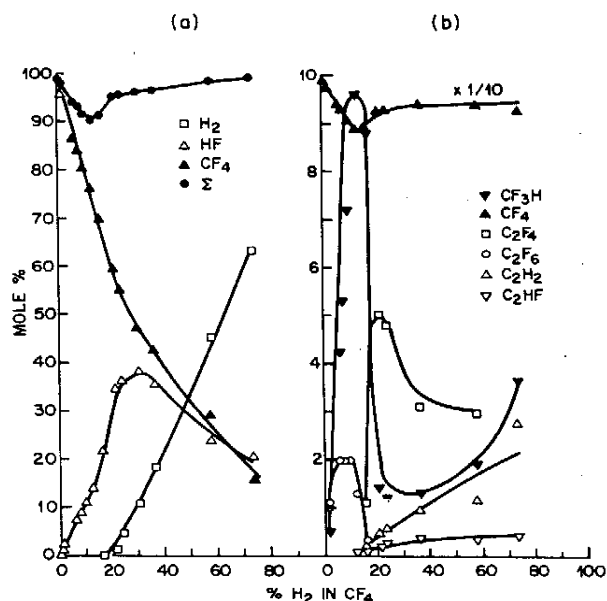


Figure 17. Mole % of the molecular species detected downstream from a  $CF_4/H_2$  discharge as a function of the  $H_2$ . (a) shows the actual composition of the gas while (b) shows the percent distribution of the carbon-containing species [36].

The addition of hydrogen molecules to  $CF_4$  leads to formation of  $HF$ , a thermodynamic sink, and produces a mixture with carbon-enriched ( $CF_3$ ,  $CF_2$ ,  $CF$ ) residues. One of the most notable observations in  $CF_4/H_2$  plasmas is the abrupt change in product distribution

and the electrical impedance of the discharge with increased  $H_2$  content, as can be seen from Fig. 17 [36]. The change in product distribution at  $H_2 > 15\%$  can be understood as the transition from a chemistry dominated by neutral  $CF_x$  species ('fluorocarbon plasma') to one dominated mainly by  $H$  atoms ('hydrogen plasma'). At low  $H_2 < 15\%$  levels, the equilibrium of the scheme ( $CF_4 \leftrightarrow CF_3 + F$ ) is upset by reactions with  $H_2$  molecules; the major hydrogen containing products are volatile  $CF_3H$  and  $HF$ . At higher  $H_2$  levels, reactions in the discharge are dominated by  $H$ -atom attack of fluorocarbons to form  $HF$  (among the fluorine abstraction reactions  $H + CF_3 \rightarrow HF + CF_2$  is the most exothermic one) with diminishing  $CF_3H$  content and increased formation of unsaturated species such as  $C_2F_4$ . These results are remarkably similar to those of the  $C_2F_6/H_2$  and  $C_2F_6/C_2H_2$  systems and suggest a similar chemistry. In these systems, residence time in the discharge zone and power density were found to control the amount of conversion of the starting materials to products [36,37]. As the ratio of  $F/C$  decreases, perfluorocarbons polymerizes readily, i.e. the balance shifts from etching to polymerization [28,35–37]. Very fast polymer formation was observed in  $C_6F_6$  and  $C_2H_2F_4$  plasmas [28]. On the other hand, hydrofluoric acid can chemically attack  $HF$ -soluble materials existing in the system.

## 7.2. Results from wire chambers

Gas mixtures based on  $CF_4$  have been widely used in semiconductor industry to etch silicon and silicon oxide substrates [32,33], therefore it was assumed that  $CF_4$  could be used in wire chambers to make a gas more resistant to aging. However, the presence of  $CF_4$  component in the gas limits the choice of construction materials for gas detectors. Decomposition of  $CF_4$  molecules in the avalanche process contaminates the gas with fluorine radicals, which may react with exposed electrode surfaces to form metal fluorides or to cause etching phenomenon. Non-gold anode wires are unacceptable for use in  $CF_4$ -based mixtures due to the formation of metal fluorides, which promote further polymer deposition in  $CF_4/iC_4H_{10}$  [22], while gold-plated wires are

considered to be inert to fluorine-based plasmas. Laboratory tests have demonstrated excellent aging properties, up to  $10 \frac{C}{cm \cdot wire}$ , of  $CF_4/iC_4H_{10}$  (80:20) avalanches, which also has an ability to etch silicon-based and hydrocarbon deposits from previously aged  $Au/W$ -wires [38,39]. However, the use of gold-plated wires does not necessarily ensure good aging properties in  $CF_4$  gases and many results show contradictory experiences with  $CF_4$ -based operation, when both polymerization and etching phenomena takes place.

Using the same experimental laboratory setup, a lack of apparent aging have been observed in  $CF_4/iC_4H_{10}$  (80:20) and  $CF_4/iC_4H_{10}$  (50:50) mixtures, whereas heavy carbonaceous deposits were found on the  $Au/W$ -wires in  $CF_4/iC_4H_{10}$  (95:5),  $CF_4/iC_4H_{10}$  (20:80) and  $CF_4/C_2H_4$  (95:5) gases [22]. Laboratory studies using radioactive sources have shown no detectable aging effects in aluminum wire chambers using  $Ar/C_2H_6/CF_4$  (48:48:4) up to  $1.0 \frac{C}{cm \cdot wire}$  [40] and in the D0 muon drift tubes filled with  $CF_4/CH_4$  (90:10) up to  $2.5 \frac{C}{cm \cdot wire}$  [41]. However, polymer deposition was observed in  $CF_4/CH_4$ -based mixtures at high ionization densities, as predicted by plasma chemistry [27]. While prototype honeycomb drift chambers had been proven to be immune to very large  $X$ -ray doses up to  $5 \frac{C}{cm \cdot wire}$  with  $CF_4/CH_4$  (80:20) mixture, severe anode and cathode aging effects were observed in hadron beams with  $Ar/CF_4/CH_4$  (74:20:6) and  $CF_4/CH_4$  (80:20) [26,42–44]. Attempts to simulate environments with large radiation doses have shown dramatical degradation of cathode foils exposed to  $Ar/CF_4/CH_4$  (74:20:6) discharge [45].

The aging properties of  $Ar(Xe)/CF_4/CO_2$  gases have been widely investigated over the last years. Using  $Ar/CF_4/CO_2$  mixtures under optimal operating conditions, no observable drop in gain due to polymerization has been found for the HERA-B honeycomb drift tubes up to  $1.5 C/cm$  [42], CMS cathode strip chambers up to  $0.4 C/cm$  [46], 13  $C/cm$  [47], LHCb straw tubes up to  $0.4 C/cm$  [45], LHCb multi-wire proportional chambers up to  $0.25 C/cm$  [48], COMPASS straw tubes up to  $1.1 C/cm$  [49] and HERMES drift tubes up to  $9 C/cm$  [50]. The main as-

set of  $CF_4$ , which prevents anode aging and allows such a long detector lifetimes, is its strong cleaning properties: etching of hydrocarbon [42] and especially *Si*-based deposits was reported for  $Ar(Xe)/CF_4/CO_2$  mixtures [47,51]. No *Si*-deposits have been observed in the irradiated region of ATLAS straw tubes for large current densities ( $> 1 \mu A/cm$ ), while *SiO/SiO<sub>2</sub>* deposits were accumulated at the edges and even outside of the irradiated area. In conclusion, the resulting balance between *Si* polymerization and  $CF_4$  etching processes was found to be very sensitive to the *Si*-source intensity and ionization density [51].

A very dangerous drawback of  $CF_4$  avalanches is a creation of harmful radicals, which have been also shown to attack and destroy electrode surfaces and construction materials. Recently, at very large current densities ( $\sim 1 - 5 \mu A/cm$ ) various manifestations of severe damage of the anode wire gold-plating in straw tubes were observed at CERN with  $Xe/CF_4/CO_2$  (70:20:10) [51] and at PNPI with  $Xe/CF_4/CO_2$  (70:20:10) and  $Ar/CF_4/CO_2$  (60:30:10) mixtures [52,53]. In honeycomb drift tubes the destruction of gold coating and even rupture of anode wires have been found in one test with  $Ar/CF_4/CO_2$  (65:30:5) [26,54]. Further studies still remain to be done to fully understand the exact mechanism of anode gold wire damage. The well-known  $CF_4$ -induced material etching phenomena is widely described as significant evaporation of *Cu* or *Al* cathode foils [40,55,56], etching of ionic conducting glass used for electrodes [57], of diamond coated glass in MSGC [58] and of glass support joints for anode wires [59].

In some cases changes of consistency of the cathode surfaces were found [22,23,60] and/or analysis of the irradiated cathodes in an  $Ar/CF_4/CO_2$  revealed the presence of fluorine-based deposits on the cathodes [46,47], which fortunately did not result in self-sustained currents. Since the resultant polymer films at cathodes could trigger breakdowns in gaseous detectors, one should seriously consider using materials in high rate detectors which are more robust to  $CF_4$ , such as gold-plated electrodes [42] or straw cathode material [51].

### 7.3. Discussion of our results

The electron-impact dissociation of  $CF_4$  in the ordinary wire avalanches near the anode may predominantly produce  $CF_3(CF_3^+)$  and  $F$  species, rather than  $CF_2$  and  $CF$ . Obviously,  $CF_3$  will not polymerize and can undergo only fragmentation or reversible dimerization reactions, while  $F$  radical is the main etchant of hydrocarbon and silicon deposits in wire chambers. Addition of hydrogen to  $CF_4$  will perturb the equilibrium ( $CF_4 \leftrightarrow CF_3 + F$ ) by scavenging  $F$  atoms and formation of stable  $HF$ . However, we believe that  $CF_4$  molecules in the  $Ar/CF_4/CH_4$  ordinary wire avalanches will not undergo a complete fragmentation: the total production rate of  $C$ ,  $CF$ ,  $CF_2$  neutral or charged species near the anode was calculated to be one order of magnitude lower than of  $CF_3$  and  $F$  [54]. This is in agreement with the reported experimental findings in  $CF_4$ /hydrocarbon mixtures [22], where no evidence of fluorocarbon polymerization has been observed.

The operation of gaseous detectors at high gas gains in presence of high ionization densities could result in greatly enhanced polymer formation due to the unavoidable appearance of sparks, glow discharges and local chamber breakdowns. This is especially relevant for the  $Ar/CF_4/CH_4$  mixtures, since due to the significant electron attachment and thus broader dynamic range of signals, the higher fraction of large amplitudes in the signal spectra at the same gas gain is expected.

Our aging studies for the HERA-B aluminum proportional chambers filled with  $Ar/CF_4/CH_4$  (74:20:6) and  $Ar/CF_4/CH_4$  (67:30:3) mixtures have shown severe anode aging and cathode surface degradation under exposure to hadron beams. SEM/EDX inspection of the aged cells in an  $Ar/CF_4/CH_4$  (67:30:3), where Malter currents were observed, revealed poorly conducting anode deposits, consisting of  $C$  and  $F$  as the only detectable elements. These results are in contrast to previous reports of polymerization of hydrocarbons in the presence of  $CF_4$  in wire chambers [22], where no fluorine deposits were incorporated into the polymer matrix.

We think that the appearance of the dark (Malter) current, due to the formation of electrically

poorly conducting polymer layer on the cathode, could be one of the main reasons of the severe anode/cathode aging in an  $Ar/CF_4/CH_4$ . Such a positive feedback between electron emission at the cathode and anode amplification and/or large charge released from heavily ionizing particles will lead to high ionization densities at distinct chamber locations. These 'Malter chains', in turn, can effect the nature and degree of  $CF_4$  and  $CH_4$  conversion in the discharge, resulting in a greatly enhanced rate of fluorine abstraction from  $CF_x$  by hydrogen and production of more low valent carbon species  $CF_2$  and  $CF$ , in accord with plasma studies reported in section 7.1. Clearly, such a change in product composition will be accompanied by an increased fluorocarbon polymerization at the same anode spots, leading to a structure of 'whisker'-type deposits. Support for this assumption also follows from the absence of anode/cathode aging when forcing chamber to breakdown in an  $Ar/CF_4$  (70:30) and from the appearance of purely carbonaceous deposits in an  $CF_4/CH_4$  (80:20), where Malter currents were not observed. The absence of aging in an  $Ar/CF_4$  also confirms that the aging in  $Ar/CF_4/CH_4$  is governed solely by the gas/phase and gas/surface reactions and appears only when  $CH_4$  is added to  $Ar/CF_4$ . Since the resistance of cathode polymer films is strongly modulated by the presence of water, this fact may explain the increased chamber lifetime in an  $Ar/CF_4/CH_4$  (67:30:3) + 1500 ppm  $H_2O$ .

Apparently,  $C_2H_2F_4/iC_4H_{10}$ -containing mixtures, usually used in RPC's, also present an interesting combination of a hydrocarbons in the presence of substantial amount of  $CF_x$  radicals. Similar to plasma polymerization, we think that the operation of wire chambers or RPC with fluorocarbon/hydrocarbon mixtures at high ionization densities in the presence of discharges and local breakdowns could result in the deposition of fluorine-based films on the electrodes, which will subsequently affect the electrode resistivity.

## 8. AGING PHENOMENA AT HIGH IONIZATION DENSITIES

Aging phenomena obviously constitutes one of the most complex and serious problems which could limit the use of gaseous detectors in severe radiation environment. After the many years of intensive research and development of radiation-hard gaseous detectors, there are a lot of contradictory experiences obtained in seemingly identical conditions, which means that we do not always control all parameters that influence the aging [30,31,61–63]. Recent experimental data from hadron beams clearly demonstrates that the initial stage of radiation tests usually performed in the laboratory may not offer the full information needed to estimate the lifetime of the real detector. The observed dependencies of aging performance at high ionization densities upon [42,64–66]:

- size of the irradiated area
- gas exchange rate
- high voltage/gas gain
- ionization density
- irradiation intensity
- particle type and energy

illustrate the need of studying the radiation hardness of the detector under conditions as close as possible to the real environment.

The dependence of the detector lifetime on the size of the irradiated area, in particular, and the increase of the aging rate in the direction of the serial gas flow means that aging should be viewed as a non-local and intensity-dependent phenomenon. These observations seem to be the most critical when trying to extrapolate the aging behavior from laboratory tests to large-scale detectors. Some of the long-lived aggressive radicals (especially  $F$ -based) may migrate for rather long time ( $\sim$  hours) in the direction of the gas flow within the irradiated area of large-scale gaseous detector and react with other avalanche produced polymer fragments. According to this picture,

this mechanism could significantly enhance polymerization in large systems, whereas in small-scale laboratory tests the aging rate typically decreases with increasing gas flow [39,40,31,64]. Due to the increased aging in the direction of the gas flow it is worthwhile to avoid gas distribution systems that supply many chambers by a serial flow. However, in closed-loop recirculation systems, which are required for detectors operated with expensive gases ( $Xe$ ,  $CF_4$ ) all impurities and reactive radical fragments will be accumulated in the gas system until they are removed by a purification system or deposited elsewhere.

The experimental dependence of chamber lifetime on high voltage, gas gain, ionization density and irradiation rate, which are also related to the total dissipated energy in the detector from ionizing particles, indicates that the aging behavior can not be predicted solely on the basis of atomic composition ratios in the mixture, without taking into account the actual operating conditions. Our studies have shown a difference of nearly two orders of magnitude in lifetime of aluminum tube chambers operated with  $Ar/CF_4/CH_4$  (74:20:6) and  $Ar/CF_4/CH_4$  (67:30:3) depending from source of irradiation and actual operating conditions and different aging performance of  $CF_4/CH_4$  (90:10) and  $Ar/CF_4/CH_4$  (67:30:3) mixtures, which have nearly identical  $F/H$  atomic ratio.

Special care has to be taken of the surface conductivity of cathodes, since it is closely related to capability of operating at large localized ionization densities. The resistivity of the microscopic non-conductive layer on the metallic cathode surface defines the maximum rate capability of the detector before the onset of electron field-emission from the cathode, which starts if the rate of ionic charge neutralization across the dielectric film is smaller than the rate of ion charge build-up [61]. Some of the metal oxide coatings on the cathode and cathode material itself may not be initially conducting enough and may impede the ion flow at high luminosities [42]. Detectors, which use insulators (RPC, MSGC, CsI) may face a new domain of aging: radiation induced increase in surface resistivity of electrodes and supporting structures due to ionic currents [61,63,68–70]. This

could trigger Malter-type breakdowns [67], which will in turn dramatically increase the polymerization rate. Several other factors may facilitate Malter current ignition, such as highly ionizing particles, sparks, sharp tips on electrodes causing corona discharges, or sporadic electron jets from microscopic dielectric insertions on cathodes [61,71]. Moreover, if the detector sparks repetitively in some weak points it might accumulate further huge charge doses locally. Since in large, mass-produced systems it is nearly impossible to avoid surface contamination of electrodes (e.g. microscopic insertions or dust particles), the polymer deposition likely starts from these localized spots and then can spread over the entire irradiated region.

Finally, in order to exclude statistical fluctuations of unknown nature and to provide a reliable estimate for the detector lifetime, the radiation tests should be carried out with several detectors irradiated under identical conditions.

## 9. CONCLUSIONS

The aging performance of the aluminum proportional chambers has been studied with  $Ar/CF_4/CH_4$  (74:20:6),  $Ar/CF_4/CH_4$  (67:30:3),  $Ar/CF_4/CO_2$  (65:30:5),  $CF_4/CH_4$  (90:10),  $CF_4/CH_4$  (80:20) and  $Ar/CF_4$  (70:30) mixtures in a variety of conditions.

Similar to plasma processing, we observed that both polymerization and etching phenomena can occur in gaseous detectors filled with  $CF_4$ /hydrocarbon gases. In particular, the aging rate in  $Ar/CF_4/CH_4$  was found to be more than two orders of magnitude higher in hadronic beams than in the laboratory studies with radioactive sources. Our experience with  $Ar/CF_4/CH_4$  mixtures also shows that the aging rate depends on the mode of operation (high voltage/gas gain) and area of irradiation (progressive deterioration of the gas gain in the direction of the serial gas flow has been observed). Given the fact that the use of  $CF_4/CH_4$ -containing gases carries a risk of anode wire aging and cathode surface degradation, due to the simultaneous polymerization of the  $CF_x$  and  $CH_x$  radicals, we have chosen the  $Ar/CF_4/CO_2$  (65:30:5) + 1000 ppm  $H_2O$  mix-

ture for the muon chamber operation.

Some practical applications of the use of  $CF_4$ -based gases in gaseous detectors were discussed. The very high aggressiveness of dissociative products of  $CF_4$  and the dynamic modification of the gas composition requires more detailed studies to evaluate the possible consequence of these effects on the long-term performance and stability of large-area gaseous detectors. The experimental data summarized here clearly indicate that the presence of large amounts of  $CF_4$  in the mixture does not necessarily ensure good aging properties automatically.

#### Acknowledgments.

We would like to thank K. Reeves (DESY/MPI Heidelberg) for reading and correcting this manuscript.

This work was partially supported by Deutsches Elektronen-Synchrotron (DESY), and by Bundesministerium für Bildung und Forschung via Max Planck Research Award.

#### REFERENCES

1. T. Lohse, et al., HERA-B, An Experiment to Study CP Violation in the B System Using an Internal Target at the HERA Proton Ring, Proposal, DESY-PRC 94/04 (1994).
2. E. Hartouni, et al., HERA-B, An Experiment to Study CP Violation in the B System Using an Internal Target at the HERA Proton Ring, Technical Design Report, DESY-PRC 95/01 (1995).
3. A. Arefiev, et al., IEEE Trans. Nucl. Sci. NS-48(4) (2001) 1059.
4. L. Christophorou, et al., Nucl. Instr. and Meth. A 163 (1979) 141.
5. L. Christophorou, et al., Nucl. Instr. and Meth. A 309 (1991) 160.
6. L. Christophorou, et al., J. Phys. Chem. Ref. Data Vol. 25(5) (1996) 1341.
7. J. Va'vra, et al., Nucl. Instr. and Meth. A 324 (1993) 113.
8. B. Schmidt, et al., Nucl. Instr. and Meth. A 273 (1988) 488.
9. J. Fischer, et al., Nucl. Instr. and Meth. A 238 (1985) 249.
10. J.E. Velazco, et al., J. Chem. Phys. Vol. 69(10) (1978) 4357.
11. A. Pansky, et al., Nucl. Instr. and Meth. A 354 (1995) 262.
12. P.G. Datskos, et al., J. Appl. Phys. Vol. 71(1) (1978) 15.
13. W.S. Anderson, et al., Nucl. Instr. and Meth. A 323 (1992) 273.
14. S. Biagi, Nucl. Instr. and Meth. A 310 (1991) 133.
15. M. Titov, Nucl. Instr. and Meth. A 446 (2000) 355.
16. M. Danilov, et al., Aging tests of the proportional wire chambers using  $Ar/CF_4/CH_4$  (74:20:6),  $Ar/CF_4/CH_4$  (67:30:3) and  $Ar/CF_4/CO_2$  (65:30:5) mixtures for the HERA-B Muon Detector, hep-ex/0107080 (2000).
17. M. Danilov, et al., Nucl. Instr. and Meth. A 494 (2002) 236.
18. A. Algeri, et al., Nucl. Instr. and Meth. A 338 (1994) 348.
19. N. Spielberg and D. Tsarnas, Rev. Sci. Instr. Vol.46 (8) (1975) 1086.
20. M. Fraga, et al., Nucl. Instr. and Meth. A 419 (1998) 485.
21. M. Danilov, et al., Aging studies of large area proportional chambers under high rate irradiation with  $CF_4$ -based mixtures, hep-ex/0111077 and hep-ex/0111078 (2001).
22. J. Wise, et al., J. Appl. Phys. Vol.74(9) (1993) 5327.
23. V. Pashhoff, Ph.D. thesis, U. Freiburg (1999).
24. M. Capeans, et al., CERN-PPE/93-136 (1993).
25. V. Bondarenko, et al., Nucl. Phys. B. Vol.44 (1995) 577.
26. A. Schreiner, Ph.D. thesis, Humboldt U., Berlin (2001).
27. H. Yasuda, these proceedings.
28. H. Yasuda, Plasma Polymerization, Academic Press (1985).
29. H.V. Boenig, Plasma Science and Technology, Cornell University Press (1982).
30. J. Va'vra, Nucl. Instr. and Meth. A 252 (1986) 547.

31. J. Kadyk, Nucl. Instr. and Meth. A 300(1991) 436.
32. M.J. Kushner, J. Appl. Phys. Vol.53(4) (1982) 2923.
33. C. Mogab, et al., J. Appl. Phys. Vol.49(7) (1978) 3796.
34. H.F. Winters, et al., J. Appl. Phys. Vol.48(12) (1977) 4973.
35. J.C. Martz, et al., J. Appl. Phys. Vol.67(8) (1990) 3609.
36. E.A. Truesdale, et al., J. Appl. Phys. Vol.50(11) (1979) 6594.
37. E.A. Truesdale, et al., J. Appl. Phys. Vol.51(5) (1980) 2909.
38. J. Kadyk, et al., IEEE Trans. Nucl. Sci. NS-37(2) (1990) 478.
39. R. Openshaw, et al., Nucl. Instr. and Meth. A 307 (1991) 298.
40. R. Openshaw, et al., IEEE Trans. Nucl. Sci. NS-36(1) (1989) 567.
41. T. Zhao, et al., IEEE Trans. Nucl. Sci. NS-49(3) (2002) 1092.
42. H. Albrecht, et al., these proceedings.
43. K. Berkhan, et al., these proceedings.
44. H. Kolanoski, Proceedings of 2000 IEEE NSS/MIC, Lyon, France (2000).
45. G. van Apeldoorn, et al., LHCb 2001-003.
46. D. Acosta, et al., these proceedings.
47. T. Ferguson, Nucl. Instr. and Meth. A 488 (2002) 240.
48. V. Souvorov, et al., these proceedings.
49. W. Dünneweber, et al., these proceedings.
50. J. Brack, et al., Nucl. Instr. and Meth. A 469 (2001) 47.
51. T. Akesson, et al., these proceedings.
52. T. Ferguson, et al., these proceedings.
53. T. Ferguson, et al., Nucl. Instr. and Meth. A 483(2002) 698 and Preprints PNPI-2406 (2001), PNPI-2443 (2001).
54. A. Schreiner, et al., these proceedings.
55. ATLAS Inner Detector TDR, CERN/LHCC/97-17 (1997).
56. K. Ecklund, et al., ICFA. Instr. Bull. Vol.12 (1996).
57. D. Marlow, talk at this workshop.
58. Y. Bagaturia, et al., Nucl. Instr. and Meth. A 490 (2002) 223.
59. M. Capeans, private communications.
60. D. Denisov, Nucl. Instr. and Meth. A 306 (1991) 200.
61. J. Va'vra, these proceedings.
62. F. Sauli, these proceedings.
63. R. Bouclier, et al., Nucl. Instr. and Meth. A 381 (1996) 289.
64. S. Kircher, et al., ATLAS-MUON-NOTE-012 (2001).
65. M. Kollefrath, talk at this workshop.
66. M. Titov, et al., IEEE Trans. Nucl. Sci. NS-49(4) (2002) 1609-1621.
67. L. Malter, Phys. Review Vol. 50 (1936) 48.
68. J. Va'vra, Comments on BaBar RPC problems and possible recovery (2002).
69. A. Breskin, Nucl. Instr. and Meth. A 371 (1996) 116.
70. J. Va'vra, Nucl. Instr. and Meth. A 371 (1996) 33.
71. P. Fonte, et al., IEEE Trans. Nucl. Sci. NS-46(3) (1999) 321.